ISSN 0735-2727, Radioelectronics and Communications Systems, 2014, Vol. 57, No. 2, pp. 92–101. © Allerton Press, Inc., 2014.
Original Russian Text © A.P. Trifonov, Yu.N. Pribytkov, 2014, published in Izv. Vyssh. Uchebn. Zaved., Radioelektron., 2014, Vol. 57, No. 2, pp. 43–54.

Stochastic Object Detection Using Its Image with Unknown Parameters in the Presence of Background[1]

A. P. Trifonov* and Yu. N. Pribytkov
Voronezh State University, Voronezh, Russia
**e-mail:* trif@phys.vsu.ru
Received in final form December 17, 2013

Abstract—A specific case where the image has the unknown area, regular component, and also the random component intensity has been considered. A maximum likelihood algorithm for the detection of stochastic image with unknown parameters was synthesized. Characteristics of the algorithm were obtained, and the impact of image characteristics and applicative background on the detection efficiency was analyzed.

DOI: 10.3103/S0735272714020046

The rapidly evolving now automatic systems of image analysis are based on multistage procedures that can include such stages as segmentation and classification of subsections of the image, the detection and discrimination of object images, and estimation of parameters. For example, one of the processing stages in a number of problems of the remote probing is the detection of objects on the basis of their images, when some or all parameters of the image are a priori unknown.

In many cases the images obtained as a result of remote probing have a stochastic structure and can be defined by a model of Gaussian random field [1, 2]. Unlike the case of thoroughly studied problems of detection of regular random signals, the processing of images involves the need of taking into account not only the additive noise, but also the background determined by the underlying surface. The presence of background can essentially affect both the image detection characteristics [3] and estimation characteristics of image parameters, such as its area [4].

The problem of detecting an image with unknown area in the presence of applicative background was considered in [3], where the regular component and the intensity of random component were assumed to be known. In a series of remote probing problems, such as detection of irregularities, the unknowns include not only the area, but also the intensity of the irregularity picture and its regular component.

The authors have considered the detection problem of a Gaussian stochastic image with unknown mathematical expectation, intensity and area observed against the Gaussian background in the continuous space with due regard for the effect of background shading. Hence, a new detection algorithm was synthesized, and asymptotic expressions for its characteristics were found.

Let us assume that random field realization $x(\mathbf{r})$ is accessible for observation owing to the remote probing in two-dimensional region G. Here $\mathbf{r} = (r_1, r_2)$ is the radius-vector of point in the plane belonging to G. Field $x(\mathbf{r})$ can include a useful image of object $s(\mathbf{r})$, spatial noise $n(\mathbf{r})$ and background radiation $\nu(\mathbf{r})$. This radiation is determined by the scattering of the probing signal by the underlying surface, on which the detectable object is located [1]. Assume that the image occupies region Ω_s with unknown area χ_0, i.e., $\Omega_s \equiv \Omega(\chi_0)$, where function $\Omega(\chi)$ defines the image shape with area χ and can be presented by using indicator

$$I(\mathbf{r},\chi) = \begin{cases} 1, & \mathbf{r} \in \Omega_s, \\ 0, & \mathbf{r} \overline{\in} \Omega_s. \end{cases}$$

[1] The study was carried out with support of RFFI (Projects Nos. 13-01-97504 and 13-08-00735).

The background shading effects occurring in practice may be taken into account by using an applicative model of image and background interaction [1]. This model allows an observed realization in the presence of image (hypothesis H_1) to be presented in the form

$$H_1: x(\mathbf{r}) = I(\mathbf{r},\chi_0)s(\mathbf{r}) + [1 - I(\mathbf{r},\chi_0)]\nu(\mathbf{r}) + n(\mathbf{r}),$$

where χ_0 is the true value of the unknown area of useful image χ that takes on its value from interval $[\chi_{min}, \chi_{max}]$. In the absence of image (hypothesis H_0) the observed realization contains only the background and spatial noise

$$H_0: x(\mathbf{r}) = \nu(\mathbf{r}) + n(\mathbf{r}).$$

Next we assume that image $s(\mathbf{r})$ and background $\nu(\mathbf{r})$ represent uniform statistically uncorrelated (mutually independent) Gaussian fields with mathematical expectations a_s, a_ν and correlation functions $B_s(\mathbf{r})$, $B_\nu(\mathbf{r})$. In addition, we shall assume that spectral densities of image

$$G_s(\boldsymbol{\omega}) = \int_{-\infty}^{\infty} B_s(\mathbf{r}) \exp(-\mathrm{j}\boldsymbol{\omega}\mathbf{r}) d\mathbf{r}$$

and background

$$G_\nu(\boldsymbol{\omega}) = \int_{-\infty}^{\infty} B_\nu(\mathbf{r}) \exp(-\mathrm{j}\boldsymbol{\omega}\mathbf{r}) d\mathbf{r}$$

are constant within the limits of regions of spatial frequencies ω_s and ω_ν, respectively. The spectral densities of image and background outside these regions are equal to zero, i.e.

$$G_s(\boldsymbol{\omega}) = g_s I(\boldsymbol{\omega}, \omega_s), \qquad G_\nu(\boldsymbol{\omega}) = g_\nu I(\boldsymbol{\omega}, \omega_\nu),$$

where $I(\boldsymbol{\omega}, \omega) = 1$, at $\boldsymbol{\omega} \in \omega$ and $I(\boldsymbol{\omega}, \omega) = 0$, at $\boldsymbol{\omega} \notin \omega$.

Let us assume that spatial noise $n(\mathbf{r})$ is uncorrelated with the image and background and represents a realization of centered white Gaussian noise with zero average and single-sided spectral density N_0.

The problem consists in detecting the image with unknown area χ, mathematical expectation a_s and normalized intensity $q_s = 2g_s / N_0$.

Now let us consider an algorithm for detecting image with unknown a_s, q_s, and χ based on the maximum likelihood method. As is known [6], this method implies the replacement of unknown values of parameters with their maximum likelihood estimates (MLE). Since MLE are the corresponding arguments of the largest value of the logarithm of likelihood ratio functional (LRF), this algorithm of detection is reduced to comparing threshold h and LRF logarithm $L(\chi, a_s, q_s)$ maximized over the set of unknown parameters:

$$L = \sup_{\chi, a_s, q_s} L(\chi, a_s, q_s) \underset{H_0}{\overset{H_1}{\gtrless}} h, \quad \chi \in [\chi_{min}, \chi_{max}].$$

An explicit form of LRF logarithm $L(\chi, a_s, q_s)$ for checking hypothesis H_1 against alternative H_0 at the known parameters of image was obtained in [5]. Extending this result to the case of unknown area, we obtain

$$L(\chi, a_s, q_s) = \frac{1}{N_0}\left\{\frac{q_s}{1+q_s} Y_{1s}(\chi) - \frac{q_\nu}{1+q_\nu} Y_{2s}(\chi) + 2\left[\frac{a_s}{1+q_s} - \frac{a_\nu}{1+q_\nu}\right] X_s(\chi)\right.$$

$$-\chi\left[\frac{a_s^2}{1+q_s}-\frac{a_\nu^2}{1+q_\nu}\right]\Bigg\}-\frac{\chi}{\chi_{\min}}\mu_s\ln[1+q_s]+\frac{\chi}{\chi_{\min}}\mu_\nu\ln[1+q_\nu], \quad (1)$$

where $X_s(\chi)=\int\limits_{\Omega(\chi)}x(\mathbf{r})d\mathbf{r}$, $Y_{is}(\chi)=\int\limits_{\Omega(\chi)}y_i^2(\mathbf{r})d\mathbf{r}$, $i=1,2$, $y_i(\mathbf{r})$ are the signals at outputs of spatial filters with transfer functions $|H_1(\boldsymbol{\omega})|^2=I(\boldsymbol{\omega},\omega_s)$, $|H_2(\boldsymbol{\omega})|^2=I(\boldsymbol{\omega},\omega_\nu)$, $q_\nu=2g_\nu/N_0$ is the normalized intensity of background, $\mu_s=\chi_{\min}S_{\omega_s}/4\pi^2$ is the number of degrees of freedom of image, $\mu_\nu=\chi_{\min}S_{\omega_\nu}/4\pi^2$ is the number of degrees of freedom of background, S_{ω_s} and S_{ω_ν} are the areas of regions ω_s and ω_ν on the frequency plane that are occupied by spectral densities of useful image $G_s(\boldsymbol{\omega})$ and background $G_\nu(\boldsymbol{\omega})$, respectively.

Maximizing relationship (1) in terms of unknown values of a_s and q_s we obtain:

$$L(\chi)=\sup_{a_s,q_s}L(\chi,a_s,q_s)=\frac{1}{N_0}\left[Y_{1s}(\chi)-\frac{q_\nu}{1+q_\nu}Y_{2s}(\chi)\right]-\frac{2}{N_0}\frac{a_\nu}{1+q_\nu}X_s(\chi)$$

$$-\frac{\chi}{2\chi_{\min}}\mu_s\left[1+\ln\left[\frac{2}{N_0}\frac{\chi_{\min}}{\chi}\frac{1}{\mu_s}\left(Y_{1s}(\chi)-\frac{X_s^2(\chi)}{\chi}\right)\right]\right]+\frac{\chi}{N_0}\frac{a_\nu^2}{1+q_\nu}+\frac{\chi}{2\chi_{\min}}\mu_\nu\ln[1+q_\nu]. \quad (2)$$

Then the algorithm of detection is reduced to the search for the absolute (largest) maximum of functional (2) and its subsequent comparison with the threshold

$$L=\sup_\chi L(\chi)\ \underset{H_0}{\overset{H_1}{\gtrless}}\ h,\quad \chi\in[\chi_{\min},\chi_{\max}].$$

Thus, the realization of the algorithm involves the need of forming three functions $Y_{1s}(\chi)$, $Y_{2s}(\chi)$, and $X_s(\chi)$ depending on the realization of observed data within the limits of region $\Omega(\chi)$ presumably occupied by the image with area χ.

The efficiency of the detection algorithm is generally characterized by the values of probabilities of false alarm error α and signal skip error β [6, 7]. By definition [6, 7] we can write

$$\alpha=P[H_1|H_0]=P[\sup_\chi L(\chi)>h|H_0]=P[L>h|H_0],$$
$$\beta=P[H_0|H_1]=P[\sup_\chi L(\chi)<h|H_1]=P[L<h|H_1],$$

where $P[H_i|H_j]$, $i,j=0,1$, designates the probability of decision-making about the truth of hypothesis H_i, while hypothesis H_j is true. Thus, the determination of α and β involves the need of finding the probabilities of the LRF logarithm (2) maximum exceeding and not exceeding the threshold h, respectively. To this end, it is necessary to have the distribution law of random quantity $L=\sup_\chi L(\chi)$ for both hypotheses H_i, $i=0,1$.

In accordance with [6–8], at $\mu_s\to\infty$ and $\mu_\nu\to\infty$ distributions of $Y_{1s}(\chi)$, $Y_{2s}(\chi)$ and LRF logarithm (1) at fixed unknown parameter χ are reduced to the Gaussian distribution. Nevertheless, the LRF logarithm (2) contains a logarithmic term of functions of the observed data; hence, the direct extension of results from papers [6–8] to the case under consideration may prove to be incorrect.

Let us consider statistical properties of this term on the assumption that the minimum area of image $\chi_{\min}$ is so large that

$$\mu_s>>1,\quad \mu_\nu>>1. \quad (3)$$

Let us introduce designation

$$A(\chi)=\frac{2}{N_0}\frac{\chi_{\min}}{\chi}\frac{1}{\mu_s}(Y_{1s}(\chi)-X_s^2(\chi)/\chi) \tag{4}$$

and present this expression in the form

$$A(\chi)=m_A(\chi)\left[1+\frac{\sigma_A(\chi)}{m_A(\chi)}\xi_A(\chi)\right],$$

at $m_A(\chi)\neq 0$, where $\xi_A(\chi)$ is the centered random process with unit dispersion, $m_A(\chi)$ and $\sigma_A^2(\chi)$ are the mathematical expectation and dispersion of $A(\chi)$. Calculating $m_A(\chi)$ and $\sigma_A^2(\chi)$ at the point of the true value of area in the absence and presence of image we obtain

$$\frac{\sigma_A(\chi_0|H_0)}{m_A(\chi_0|H_0)}=\frac{1}{\sqrt{\mu_s}}\frac{\sqrt{2\dfrac{\chi_{\min}}{\chi_0}\left[(1+q_{\nu 0})^2\left(\sqrt{\dfrac{\mu_\nu}{\mu_s}}\varphi-\dfrac{\chi_{\min}}{\chi_0\mu_s}\right)+1-\sqrt{\dfrac{\mu_\nu}{\mu_s}}\varphi\right]}}{\left[(1+q_{\nu 0})\left(\sqrt{\dfrac{\mu_\nu}{\mu_s}}\varphi-\dfrac{\chi_{\min}}{\chi_0\mu_s}\right)+1-\sqrt{\dfrac{\mu_\nu}{\mu_s}}\varphi\right]},$$

$$\frac{\sigma_A(\chi_0|H_1)}{m_A(\chi_0|H_1)}=\sqrt{\frac{2}{\mu_s\dfrac{\chi_0}{\chi_{\min}}-1}}, \tag{5}$$

where $\varphi=S_{\omega_{s\nu}}/\sqrt{S_{\omega_s}S_{\omega_\nu}}$ is the coefficient determining the degree of overlapping of regions occupied by spectral densities of useful image and background, $S_{\omega_{s\nu}}$ is the overlapping area of these regions.

From expression (5) it follows that at $\mu_s\to\infty$ ratio $\sigma_A(\chi_0)/m_A(\chi_0)\to 0$ for both hypotheses. More cumbersome calculations make it possible to obtain a similar result for any $\chi\in[\chi_{\min},\chi_{\max}]$. Then, assuming condition (3) is satisfied, similar to paper [7] the following approximate equality can be used:

$$\ln A(\chi)\approx\ln m_A(\chi)+\frac{\sigma_A(\chi)}{m_A(\chi)}\xi_A(\chi)=\ln m_A(\chi)+\frac{A(\chi)}{m_A(\chi)}-1. \tag{6}$$

Substituting expression (6) into (2) with due regard for (4) we obtain

$$L(\chi)\approx\frac{1}{N_0}\left[\frac{m_A(\chi)-1}{m_A(\chi)}Y_{1s}(\chi)-\frac{q_\nu}{1+q_\nu}Y_{2s}(\chi)\right]-\frac{2}{N_0}\frac{a_\nu}{1+q_\nu}X_s(\chi)$$

$$+\frac{1}{N_0}\frac{X_s^2(\chi)}{\chi m_A(\chi)}+\frac{\chi}{N_0}\frac{a_\nu^2}{1+q_\nu}-\frac{\chi}{2\chi_{\min}}\mu_s\ln m_A(\chi)+\frac{\chi}{2\chi_{\min}}\mu_\nu\ln[1+q_\nu]. \tag{7}$$

Let us designate the mathematical expectation and dispersion of the Gaussian process $X_s(\chi)$ as $m_{Xs}(\chi)$ and $\sigma_{Xs}^2(\chi)$, respectively. Then, substituting expression $X_s(\chi)=m_{Xs}(\chi)+\sigma_{Xs}(\chi)\xi_{Xs}(\chi)$ into (7), we obtain

$$L(\chi)\approx L_G(\chi)+D(\chi)\xi_{Xs}^2(\chi),$$

where

$$L_G(\chi)=\frac{1}{N_0}\left[\frac{m_A(\chi)-1}{m_A(\chi)}Y_{1s}(\chi)-\frac{q_\nu}{1+q_\nu}Y_{2s}(\chi)\right]+2X_s(\chi)\frac{1}{N_0}\left(\frac{1}{\chi}\frac{m_{Xs}(\chi)}{m_A(\chi)}-\frac{a_\nu}{1+q_\nu}\right)$$

$$-\frac{\chi}{N_0}\left(\frac{1}{\chi}\frac{m_{Xs}^2(\chi)}{m_A(\chi)}-\frac{a_\nu^2}{1+q_\nu}\right)-\frac{\chi}{2\chi_{\min}}\mu_s\ln m_A(\chi)+\frac{\chi}{2\chi_{\min}}\mu_\nu\ln\left[1+q_\nu\right], \quad (8)$$

$L_G(\chi)$ is the asymptotic Gaussian (at $\mu_s\to\infty$ and $\mu_\nu\to\infty$) component of the LRF algorithm, $\xi_{Xs}(\chi)$ is the Gaussian random process with zero average and unit dispersion $D(\chi)=\sigma_{Xs}^2(\chi)/[\chi N_0 m_A(\chi)]$.

Thus, if conditions (3) are fulfilled, LRF algorithm (2) can be approximated by a sum of Gaussian process $L_G(\chi)$ and process $D(\chi)\xi_{Xs}^2(\chi)$, the values of which obey the gamma distribution. Let us consider the first two moments of both terms.

After the calculation of dispersion $\sigma_{Xs}^2(\chi)$ and mathematical expectation $m_A(\chi)$ for both hypotheses, we obtain the following expressions for $D(\chi)$:

$$D(\chi\mid H_1)=\left[\frac{\min(\chi_0,\chi)}{\chi}(1+q_{s0})+\left[1-\frac{\min(\chi_0,\chi)}{\chi}\right](1+q_\nu)\right]$$

$$\times\left[1+\frac{\min(\chi_0,\chi)}{\chi}q_{s0}-\sqrt{\frac{\mu_\nu}{\mu_s}}\varphi\left[1-\frac{\min(\chi_0,\chi)}{\chi}\right]q_\nu\right.$$

$$-\frac{\chi_{\min}}{\chi}\frac{1}{\mu_s}\left[\left(\frac{\min(\chi_0,\chi)}{\chi}(1+q_{s0})+\left[1-\frac{\min(\chi_0,\chi)}{\chi}\right](1+q_\nu)\right)+a_{s0}^2\frac{2}{N_0}\min(\chi_0,\chi)\right.$$

$$\left.\left.+a_\nu^2\frac{2}{N_0}\left[\chi-\min(\chi_0,\chi)\right]-\frac{1}{\chi}\frac{2}{N_0}\left(a_{s0}\min(\chi_0,\chi)+a_\nu\left[\chi-\min(\chi_0,\chi)\right]\right)^2\right]\right]^{-1},$$

$$D(\chi|H_0)=(1+q_{\nu0})\left[1+\sqrt{\mu_\nu/\mu_s}\varphi q_{\nu0}-\chi_{\min}(1+q_\nu)/(\chi\mu_s)\right]^{-1}.$$

Using approximation (3) we can find expressions for mathematical expectations m_{L_G} and correlation functions B_{L_G} of LRF logarithm $L_G(\chi)$ (7):

for hypothesis H_1

$$m_{L_G}(\chi|H_1)=\left(\min(\chi,\chi_0)k_1+\left[\chi-\min(\chi,\chi_0)\right]k_2\right)/\chi_0,$$

$$B_{L_G}(\chi_1,\chi_2|H_1)=\left(\min(\chi_0,\chi_1,\chi_2)d_1+\left[\min(\chi_1,\chi_2)-\min(\chi_0,\chi_1,\chi_2)\right]d_2\right)/\chi_0$$

$$-c_2\left(\max(\chi_1,\chi_0)+\max(\chi_2,\chi_0)-2\chi_0\right)/\chi_0,$$

for hypothesis H_0

$$m_{L_G}(\chi|H_0)=k\chi/\chi_0,$$

$$B_{L_G}(\chi_1,\chi_2|H_0)=c_1\min(\chi_1,\chi_2)/\chi_0,$$

where

$$k_1=\frac{1}{2}\frac{\chi_0}{\chi_{\min}}\left[\mu_s q_{s0}-\mu_\nu\frac{q_\nu}{1+q_\nu}-\sqrt{\mu_s\mu_\nu}\varphi q_{s0}\frac{q_\nu}{1+q_\nu}+\frac{2}{N_0}\chi_0\frac{[a_{s0}-a_\nu]^2}{1+q_\nu}+\mu_\nu\ln[1+q_\nu]-\mu_s\ln[1+q_{s0}]\right],$$

$$k_2=\frac{1}{2}\frac{\chi_0}{\chi_{\min}}\left[\mu_s\frac{q_{s0}}{1+q_{s0}}-\mu_\nu q_\nu-\sqrt{\mu_s\mu_\nu}\varphi q_\nu\frac{q_{s0}}{1+q_{s0}}-\frac{2}{N_0}\chi_0\frac{[a_{s0}-a_\nu]^2}{1+q_{s0}}+\mu_\nu\ln[1+q_\nu]-\mu_s\ln[1+q_{s0}]\right],$$

$$k=\frac{1}{2}\frac{\chi_0}{\chi_{\min}}\left\{\mu_s\frac{\sqrt{\frac{\mu_\nu}{\mu_s}}\varphi q_\nu}{1+\sqrt{\frac{\mu_\nu}{\mu_s}}\varphi q_\nu}-\mu_\nu q_\nu-\sqrt{\mu_s\mu_\nu}\varphi q_\nu\frac{\sqrt{\frac{\mu_\nu}{\mu_s}}\varphi q_\nu}{1+\sqrt{\frac{\mu_\nu}{\mu_s}}\varphi q_\nu}+\mu_\nu\ln\big[1+q_\nu\big]-\mu_s\ln\left[1+\sqrt{\frac{\mu_\nu}{\mu_s}}\varphi q_\nu\right]\right\},$$

$$d_1=\frac{1}{2}\frac{\chi_0}{\chi_{\min}}\left\{\mu_s q_{s0}^2+\mu_\nu\left[\frac{q_\nu}{1+q_\nu}\right]^2+\sqrt{\mu_s\mu_\nu}\varphi\left(\left[\frac{q_{s0}-q_\nu}{1+q_\nu}\right]^2-\left[\frac{q_\nu}{1+q_\nu}\right]^2-q_{s0}^2\right)+\frac{4\chi_{\min}}{N_0}(a_{s0}-a_\nu)^2\frac{1+q_{s0}}{(1+q_\nu)^2}\right\},$$

$$d_2=\frac{1}{2}\frac{\chi_0}{\chi_{\min}}\left\{\mu_s\left(\frac{q_{s0}}{1+q_{s0}}\right)^2+\mu_\nu q_\nu^2+\sqrt{\mu_s\mu_\nu}\varphi\left(\left(\frac{q_{s0}-q_\nu}{1+q_{s0}}\right)^2-\left(\frac{q_{s0}}{1+q_{s0}}\right)^2-q_\nu^2\right)+\frac{4\chi_{\min}}{N_0}(a_{s0}-a_\nu)^2\frac{1+q_\nu}{(1+q_{s0})^2}\right\}$$

,

$$c_1=\frac{1}{2}\frac{\chi_0 q_\nu^2}{\chi_{\min}(1+\sqrt{\mu_\nu/\mu_s}\varphi q_\nu)^2}\left\{\mu_s\left(\sqrt{\mu_\nu/\mu_s}\varphi\right)^2+\mu_\nu q_\nu^2+\sqrt{\mu_s\mu_\nu}\varphi q_\nu^2\right.$$

$$\left.\times\left(\left(1-\sqrt{\mu_\nu/\mu_s}\varphi\right)^2-\left(\sqrt{\mu_\nu/\mu_s}\varphi\right)^2-1\right)+\frac{2\chi_{\min}}{N_0}\frac{(1-\sqrt{\mu_\nu/\mu_s}\varphi)^2}{[1+q_\nu]}\left(a_{s0}-a_\nu\right)^2\right\},$$

$$c_2=\frac{1}{2}\frac{\chi_0}{\chi_{\min}}\left\{\left(\mu_s\frac{q_{s0}}{1+q_{s0}}-\sqrt{\mu_s\mu_\nu}\varphi\frac{q_\nu}{1+q_\nu}\right)\left(q_{s0}+\sqrt{\frac{\mu_\nu}{\mu_s}}\varphi q_\nu\right)+\frac{2}{N_0}\chi_{\min}\frac{1+q_\nu}{(1+q_{s0})^2}(a_{s0}-a_\nu)^2\right\}, \quad (9)$$

Comparing these characteristics with characteristics of LRF logarithm (1), obtained in [3], it can be shown that in the presence of image we have:

$$m_{L_G}(\chi|H_1)\approx m_L(\chi|H_1),$$

$$B_{L_G}(\chi_1,\chi_2|H_1)\approx B_L(\chi_1,\chi_2|H_1)-c_2(\max(\chi_1,\chi_0)+\max(\chi_2,\chi_0)-2\chi_0)/\chi_0,$$

where $m_L(\chi|H_1)$, $B_L(\chi_1,\chi_2|H_1)$ are the mathematical expectation and correlation function of LRF logarithm (1) obtained at the a priori known values of a_s and q_s.

Using the obtained expressions we shall compare the behavior of the dispersion of Gaussian component $D_{L_G}(\chi_0|H_i)=B_{L_G}(\chi_0,\chi_0|H_i)$, $i=0,1$ and quantity $D(\chi_0)$ at $\mu_s\to\infty$ and $\chi=\chi_0$. If the received realization of observed data contains image, the dispersion of the Gaussian component of LRF logarithm has the form

$$D_{L_G}(\chi_0|H_1) = \chi d_1 / \chi_0.$$

From expression (9) it follows that with unlimited rise of the number of degrees of freedom of the image and background $d_1 \to \infty$ if the intensities of random components of image q_{s0} and background q_ν are non-zero. Parameter $D(\chi_0|H_1) = [1 - \chi_{\min} / \chi_0 \mu_s]^{-1} \to 1$ at $\mu_s \to \infty$. Hence, it follows that given hypothesis H_1 the contribution of non-Gaussian component of the LRF logarithm decreases with the rise of the number of degrees of freedom of μ_s and μ_ν.

A similar conclusion can be also made in the absence of image, because $D_{L_G}(\chi_0|H_0) = c_1 \to \infty$ at $\mu_\nu \to \infty$ and $q_\nu \neq 0$, while parameter $D(\chi_0|H_0)$ tends to a finite quantity:

$$D(\chi_0|H_0) \to (1 + q_\nu)[1 + \sqrt{\mu_\nu / \mu_s}\varphi q_\nu]^{-1} \leq (1 + q_\nu)$$

at $\mu_\nu \to \infty$ and $\mu_s \to \infty$.

That is why at $q_{s0} > 0$, $q_\nu > 0$, and fulfillment of condition (3), the non-Gaussian component of LRF logarithm can be neglected by assuming $L(\chi) \approx L_G(\chi)$. Thus, we can find characteristics of the detection algorithm in Gaussian approximation.

Comparing LRF logarithms $L_G(\chi)$ (8) and $L(\chi, a_s, q_s)$ (1) we may conclude that these expressions have the same structure and differ only by their determinate terms and also coefficients of random functions $Y_{1s}(\chi)$, $Y_{2s}(\chi)$, and $X_s(\chi)$. As was shown in [3], in the neighborhood of true value of parameter χ_0 LRF logarithm $L(\chi, a_s, q_s)$ (1) can be approximated by the Gaussian Markov process. Hence, $L(\chi) \approx L_G(\chi)$ can be also considered as Gaussian Markov process in the neighborhood of the true value of area χ_0. Therefore, the complete, in statistical sense, description of LRF logarithm $L(\chi)$ involves the need of determining the initial probability density and transition probability [8].

In the case under consideration the initial probability density will be the univariate probability density of LRF logarithm at $\chi = \chi_{\min}$. Since $L(\chi)$ is an asymptotically Gaussian process, if condition (3) is satisfied, the initial probability density has the form:

$$W(L, \chi_{\min}|H_i) = \frac{1}{\sigma_{L_G}(\chi_{\min}|H_i)\sqrt{2\pi}} \exp\left\{-\frac{\left(L - m_{L_G}(\chi_{\min}|H_i)\right)^2}{2\sigma^2_{L_G}(\chi_{\min}|H_i)}\right\}, \tag{10}$$

where $\sigma^2_{L_G}(\chi_{\min}|H_i) = B_{L_G}(\chi_{\min}, \chi_{\min}|H_i)$, $i = 0, 1$.

The calculation of the transition probability implies the need of finding the drift coefficient

$$M_1(\chi) = \lim_{\Delta\chi \to 0+} \langle [L_{1G}(\chi + \Delta\chi) - L_{1G}(\chi)] | L_{1G}(\chi) \rangle / \Delta\chi$$

and diffusion coefficient of LRF logarithm $L(\chi)$

$$M_2(\chi) = \lim_{\Delta\chi \to 0+} \langle [L_{1G}(\chi + \Delta\chi) - L_{1G}(\chi)]^2 | L_{1G}(\chi) \rangle / \Delta\chi$$

in the neighborhood of the true value of area, where $|\chi - \chi_0|/\chi_0 << 1$. It can be shown that if the image intensity is non-zero, while area χ_0 is so large that apart from condition (3) the following conditions are fulfilled:

$$\mu_s >> \max\left(\{1 + 1/q_{s0}\},\ \{|q_{s0} - q_\nu|\}, \{2\chi_0(a_{s0} - a_\nu)^2 / [\min(1, q_{s0})N_0]\}\right)\chi_{\min} / \chi_0,$$

then the desired coefficients have the form:

for hypothesis H_1

$$M_1(\chi \mid H_1) = \frac{1}{\chi_{\min}} \begin{cases} k_1, & \chi_{\min} \le \chi \le \chi_0, \\ -k_2, & \chi_0 < \chi \le \chi_{\max}, \end{cases}$$

$$M_2(\chi \mid H_1) = \frac{1}{\chi_{\min}} \begin{cases} d_1, & \chi_{\min} \le \chi \le \chi_0, \\ d_2, & \chi_0 < \chi \le \chi_{\max}, \end{cases} \tag{11}$$

for hypothesis H_0

$$M_1(L|H_0) = -k / \chi_{\min},$$

$$M_2(L|H_0) = c_1 / \chi_{\min}. \tag{12}$$

Solving the Fokker–Planck–Kolmogorov equations with coefficients (11) and (12) at the initial (10) and relevant boundary conditions, similar to [7], we can find the probabilities of the false alarm and signal skip:

$$\alpha(h) = 1 - \frac{1}{\sqrt{2\pi}} \int_0^\infty \exp\left[-\frac{\left(x - h_1 - \hat{z}_N\right)^2}{2} \right] \left\{ \Phi\left(\hat{z}_N \sqrt{\frac{\chi_{\max} - \chi_{\min}}{\chi_{\min}}} + x \sqrt{\frac{\chi_{\min}}{\chi_{\max} - \chi_{\min}}} \right) \right.$$

$$\left. - \exp(-2x\hat{z}_N) \Phi\left(\hat{z}_N \sqrt{\frac{\chi_{\max} - \chi_{\min}}{\chi_{\min}}} - x \sqrt{\frac{\chi_{\min}}{\chi_{\max} - \chi_{\min}}} \right) \right\} dx, \tag{13}$$

$$\beta(h) = \frac{1}{\sqrt{2\pi}} \int_0^\infty \exp\left[-\frac{(x + z_1)^2 + h_2^2 - 2h_2 z_1}{2} \right] \left\{ \Phi\left(z_N \sqrt{\frac{\chi_{\max} - \chi_0}{\chi_{\min}}} + xC \sqrt{\frac{\chi_0}{\chi_{\max} - \chi_0}} \right) \right.$$

$$\left. - \exp\left(-2xCz_N \sqrt{\frac{\chi_0}{\chi_{\min}}} \right) \Phi\left(z_N \sqrt{\frac{\chi_{\max} - \chi_0}{\chi_{\min}}} - xC \sqrt{\frac{\chi_0}{\chi_{\max} - \chi_0}} \right) \right\}$$

$$\times \left\{ \exp(xh_2) \Phi\left(h_2 \sqrt{\frac{\chi_0 - \chi_{\min}}{\chi_{\min}}} + x \sqrt{\frac{\chi_{\min}}{\chi_0 - \chi_{\min}}} \right) \right.$$

$$\left. - \exp(-xh_2) \Phi\left(h_2 \sqrt{\frac{\chi_0 - \chi_{\min}}{\chi_{\min}}} - x \sqrt{\frac{\chi_{\min}}{\chi_0 - \chi_{\min}}} \right) \right\} dx, \tag{14}$$

where the following designations are used:

$$h_1 = h / \sqrt{d_2}, \quad \hat{z}_N^2 = k^2 / c_1,$$

$$z_1^2 = k_1^2 \chi_0 / d_1 \chi_{\min}, \quad h_2 = h\sqrt{\chi_{\min} / d_1 \chi_0}, \quad C^2 = d_1 / d_2,$$

$\Phi(y) = \int_{-\infty}^{y} \exp(-x^2/2) dx \Big/ \sqrt{2\pi}$ is the probability integral.

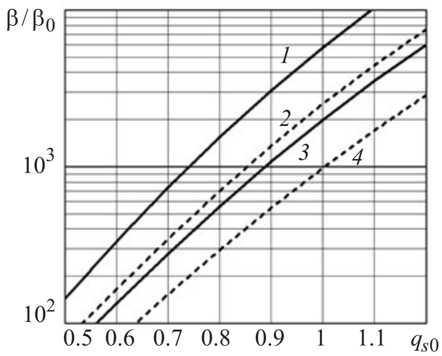

Fig. 1.

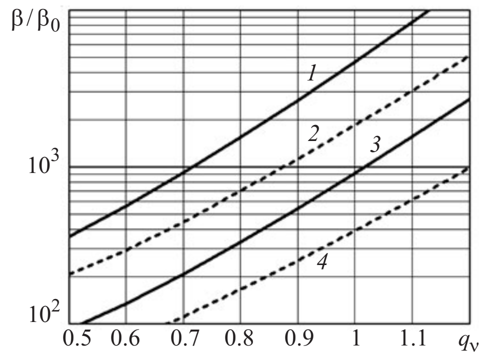

Fig. 2.

The resultant expressions make it possible to analyze the performance efficiency of the maximum likelihood algorithm for different statistical characteristics of useful image and background, and also to determine the degree of influence of their difference on the detection efficiency.

The signal skip probability (14) obtained at unknown χ, a_s, and q_s coincides with the signal skip probability obtained in [3] for the unknown area and a priori known values of a_s and q_s. Hence, we can make a conclusion that in case condition (3) is satisfied, the lack of knowledge of mathematical expectation a_s and the relative intensity of image q_s does not asymptotically affect the signal skip probability. Thus, the difference in efficiency of detecting the image with unknown parameters a_s and q_s as compared with the case of known a_s and q_s is determined by the rise of the false alarm probability.

For estimating this difference we shall use the Neumann–Pearson criterion [6], which implies that threshold h in formulas (13) and (14) is determined from the specified false alarm probability ε, i.e., it is a solution of equation:

$$\alpha(h) = \varepsilon. \tag{15}$$

The numerical solution of this equation gives the value of threshold $\hat{h}$; substituting the latter into expression (14) we find the value of signal skip probability $\beta = \beta(\hat{h})$ at unknown parameters a_s and q_s. For the case of known a_s and q_s we substitute into formula (15) the expression for false alarm $\alpha(h, a_s, q_s)$ obtained in [3] in place of $\alpha(h)$ (13).

Let $\hat{h}_0$ be the threshold obtained by numerical solution of equation $\alpha(h, a_s, q_s) = \varepsilon$. Then substituting $\hat{h}_0$ into formula (14) we obtain an appropriate value of signal skip $\beta_0 = \beta(\hat{h}_0)$ for the case of known a_s and q_s.

The relationships of the relative rise of signal skip probability β / β_0 as a function of the true value of the relative intensity of image q_{s0} at the fixed value of false alarm $\varepsilon = 10^{-3}$ and different values of the relative intensity of background q_ν are presented by solid lines in Fig. 1. These curves were plotted on the assumption that the spectral densities of image and background do not overlap so that $\varphi = 0$. In addition, these relationships were plotted for the following selected parameters: $\chi_0 = 0.5\chi_{\max}$, $\chi_{\min} = 0.1\chi_{\max}$, $a_{s0} = a_\nu$, $\mu_s = \mu_\nu = 200$. Curves *1* and *2* were calculated at $q_\nu = 0.8$, and curves *3* and *4* at $q_\nu = 0.6$.

Dashed curves in Fig. 1 correspond to the false alarm probability $\varepsilon = 10^{-4}$.

Figure 2 presents the relationships of the loss of β / β_0 as a function of background intensity q_ν at different values of image intensity q_{s0} under the same conditions as above. In this case solid lines correspond to the false alarm probability $\varepsilon = 10^{-3}$, while dashed ones correspond to $\varepsilon = 10^{-4}$. Curves *1* and *2* were calculated at $q_{s0} = 0.8$ and curves *3* and *4* at $q_{s0} = 0.6$.

The analysis of curves (Figs. 1, 2) reveals that the lack of knowledge of true values of image parameters a_s and q_s can lead to a significant loss in the efficiency of object detection by using its image. Moreover, if the spectral densities of image and background occupy nonoverlapping regions on the plane of spatial frequencies, the specified relative loss increases both with the rise of relative intensity of interfering background q_ν and with the rise of true value of the relative intensity of useful image q_{s0}. However, with the reduction of the required probability of false alarm the relative loss decreases.

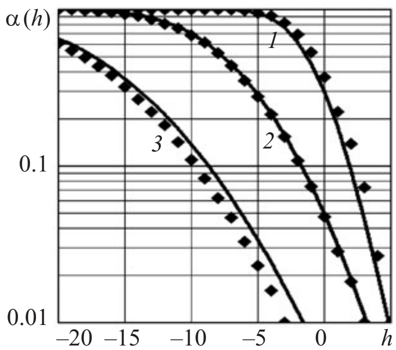

Fig. 3.

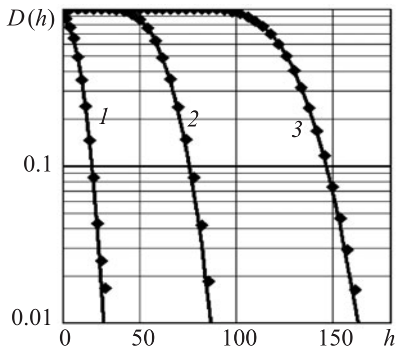

Fig. 4.

Statistical simulation was conducted for the purpose of verification of the detection algorithm and establishing the application boundaries of the obtained asymptotic analytical expressions for the detection characteristics. The simulation was performed on the assumption that the image represents a square with area $\chi_0 = 4\chi_{\min}$, while the range of possible values of unknown area is equal to $\chi_{\max} / \chi_{\min} = 9$. Mathematical expectations and intensities of image and background were selected equal: $a_s = a_\nu = 0$ and $q_s = q_\nu = q$, hence, the detection was performed at the expense of the difference of spectral characteristics of image mad background. In this case the regions occupied by spectral densities of image and background were selected of rectangular shape. The degree of overlapping of these regions was characterized by coefficient $\varphi = 0.1$.

Figures 3 and 4 present the relationships of the false alarm probability $\alpha(h)$ (Fig. 3) and correct detection $D(h) = 1 - \beta(h)$ (Fig. 4) as a function of threshold h at $\mu_s = \mu_\nu = \mu = 10^3$. Solid lines show the relationships calculated by using formulas (13) and (14), while diamonds designate the simulation results for appropriate parameters. Curves *1*, *2*, and *3* were calculated at q = 0.1, 0.2, 0.3, respectively. Figure 3 indicates satisfactory agreement of the calculation results by formula (13) and the simulation results. Correspondingly, Fig. 4 shows that the signal skip probability (14) (or correct detection) obtained for the case of known parameters a_s and q_s satisfactorily describes the synthesized maximum likelihood algorithm at unknown parameters a_s, q_s and $\mu >> 1$.

Thus, a structure of the maximum likelihood algorithm for detection of stochastic image with unknown area, mathematical expectation, and intensity was obtained. The algorithm characteristics were found. It was shown that at sufficiently large values of the number of degrees of freedom for image and background the lack of knowledge of the intensity and mathematical expectation of image mostly affects the probability of false alarm errors, while the signal skip probabilities are asymptotically equal both with the known and unknown parameters of image. The statistical simulation of the detection algorithm was conducted for performance verification of the algorithm and corroboration of the results obtained.

REFERENCES

1. A. A. Bychkov and V. A. Pon'kin, "Detection of images of spatially extended objects shading the background," Avtometriya, No. 4, 33 (1992).
2. G. I. Peretyagin, "Representation of images using the Gaussian random fields," Avtometriya, No. 6, 42 (1984).
3. A. P. Trifonov and Yu. N. Pribytkov, "Detection of objects with unknown area in the presence of background," Avtometriya **41**, No. 3, 24 (2005).
4. A. P. Trifonov, Yu. N. Pribytkov, "Area estimation of stochastic objects from an image containing a background," Optoelectron. Instrum. Data Process. **46**, No. 2, 142 (2010). DOI: 10.3103/S8756699010020056.
5. A. P. Trifonov and Yu. N. Pribytkov, "The detection of stochastic image with unknown parameters," Izv. Vyssh. Uchebn. Zaved., Radioelektron. **45**(9), 10 (2002) [Radioelectron. Commun. Syst. **45**(9), 8 (2002)].
6. P. S. Akimov, P. A. Bakut, V. A. Bogdanovich, et al., *Theory of Signal Detection* (Radio i Svyaz', Moscow, 1984) [in Russian, ed. by P. A. Bakut].
7. A. P. Trifonov, E. P. Nechaev, and V. I. Parfenov, *Detection of Stochastic Signals with Unknown Parameters* (VGU, Voronezh, 1991) [in Russian, ed. by A. P. Trifonov].
8. V. I. Tikhonov and M. A. Mironov, *Markov Processes* (Radio i Svyaz', Moscow, 1977) [in Russian].